

A Combined Experimental and Computational Study of Dihydrido(phosphinooxazoline)iridium Complexes

Clément Mazet, Sebastian P. Smidt, Markus Meuwly,* and Andreas Pfaltz*

Contribution from the Departments of Organic Chemistry, St. Johannis Ring 19, and Physical Chemistry, Klingelbergstrasse 80, Basel University, CH-4056 Basel, Switzerland

Received June 22, 2004; E-mail: Andreas.Pfaltz@unibas.ch; m.meuwly@unibas.ch

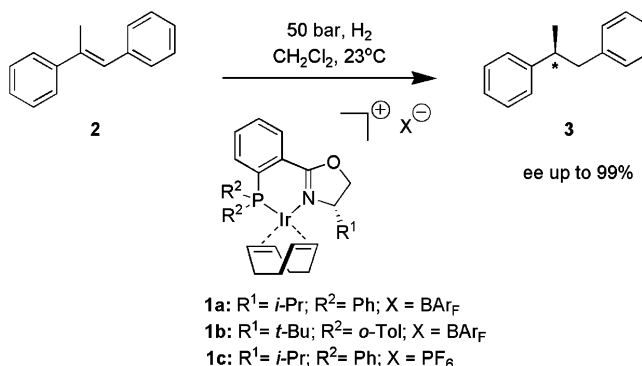
Abstract: The reaction of a [(PHOX)Ir(COD)]⁺ complex (COD = 1,5-cyclooctadiene) with dihydrogen was studied by NMR spectroscopy (PHOX = chiral phosphinooxazoline ligand). A single [(PHOX)Ir(H)₂(COD)]⁺ isomer was formed as the primary product at -40 °C in THF. Subsequent reaction with H₂ at -40 to 0 °C led to a mixture of two diastereomeric [(PHOX)Ir(H)₂(solvent)₂]⁺ complexes with concomitant loss of cyclooctane. The stereochemistry of the three hydride complexes could be assigned from the NMR data. The structures and energies of the observed hydride complexes and the possible stereoisomers were calculated using density functional theory. The substantial energy differences (up to 39 kcal/mol) between the various stereoisomers demonstrate the strong influence of the chiral ligand. The observed stereoselective formation of dihydride complexes can be explained by steric effects of the PHOX ligand combined with a strong electronic influence of the coordinating N and P atoms, favoring addition of a hydride *trans* to the Ir–N bond.

Introduction

Iridium complexes derived from chiral *P,N*-ligands have emerged as a new class of catalysts that has considerably enhanced the scope of asymmetric olefin hydrogenation. In contrast to rhodium and ruthenium phosphine catalysts, they do not require a polar coordinating group next to the C=C bond for high activity and enantioselectivity. In addition to unfunctionalized alkenes, high enantiomeric excesses were also obtained with various functionalized olefins for which no suitable chiral catalysts were available before.¹

Our initial work focused on iridium complexes derived from chiral phosphinooxazoline (PHOX) ligands.² These complexes can be viewed as chiral analogues of the Crabtree catalyst that is known for its unusual reactivity toward tris- and tetrasubstituted unfunctionalized alkenes.³ With complex **1b** excellent enantioselectivities, high rates, and turnover numbers of up to 5000 were achieved in the hydrogenation of trisubstituted olefins such as **2** (Scheme 1). A subsequent systematic search for other suitable *P,N*-ligands has led to several new catalysts that give high enantioselectivities with a wide variety of functionalized and unfunctionalized olefins.^{1,4} It was necessary to screen a large number of different ligands because no mechanistic model, rationalizing the observed enantioselectivities, was available. Thus, for future work it would be desirable to gain better

Scheme 1. Asymmetric Hydrogenation of (*E*)-1,2-Diphenyl-1-propene Catalyzed by Chiral (Phosphinooxazoline)iridium Complexes (BAR_F = Tetrakis[3,5-bis(trifluoromethyl)phenyl]borate)



mechanistic insight that allows a more rational approach to catalyst development.

Crabtree has convincingly demonstrated that the reactivity of iridium complexes is strikingly different from that of analogous rhodium complexes.^{3c} Therefore, it is dangerous to draw conclusions concerning the mechanism of iridium-catalyzed asymmetric hydrogenation from analogous rhodium-catalyzed reactions, which are mechanistically well understood.^{5,6} The electrophilic nature of the cationic iridium catalysts seems to be essential for the observed high reactivity toward tri- and tetrasubstituted alkenes. Thus, for high catalytic activity,

(1) For a recent review, see: Pfaltz, A.; Blankenstein, J.; Hilgraf, R.; Hörmann, E.; McIntyre, S.; Menges, F.; Schönleber, M.; Smidt, S. P.; Wüstenberg, B.; Zimmermann, N. *Adv. Synth. Catal.* **2003**, *345*, 33–43.
 (2) Lightfoot, A.; Schnider, P.; Pfaltz, A. *Angew. Chem., Int. Ed.* **1998**, *37*, 2897–2899.
 (3) (a) Crabtree, R. H.; Felkin, H.; Morris, G. E. *J. Chem. Soc., Chem. Commun.* **1976**, 716–717. (b) Crabtree, R. H.; Felkin, H.; Morris, G. E. *J. Organomet. Chem.* **1977**, *141*, 205–215. (c) Crabtree, R. H. *Acc. Chem. Res.* **1979**, *12*, 331–338.

(4) (a) Drury, W. J., III; Zimmermann, N.; Keenan, M.; Hayashi, M.; Kaiser, S.; Goddard, R.; Pfaltz, A. *Angew. Chem., Int. Ed.* **2004**, *43*, 70–74. (b) Smidt, S. P.; Menges, F.; Pfaltz, A. *Org. Lett.* **2004**, *6*, 2023–2026. See also: (c) Bunlaksanusorn, T.; Polborn, K.; Knochel, P. *Angew. Chem., Int. Ed.* **2003**, *42*, 3941–3943. (d) Liu, D.; Tang, W.; Zhang, X. *Org. Lett.* **2004**, *6*, 513–516. (e) Perry, M. C.; Powell, M. T.; Cui, X.; Hou, D.-R.; Reibenspies, J. H.; Burgess, K. *J. Am. Chem. Soc.* **2003**, *125*, 113–123.

coordinating solvents or anions must be avoided. In our case, dichloromethane and tetrakis[3,5-(trifluoromethyl)phenyl]borate (BAR_{F}) as a bulky, very weakly coordinating anion proved to be a good choice. Cyclooctadiene complexes such as **1a** or **1b**, which are used as precatalysts, are air- and moisture-stable compounds, the structures of which are known in detail from X-ray and NMR analyses. However, the catalytically active complexes, formed after dissociation of cyclooctadiene upon treatment with dihydrogen, are highly reactive, short-lived species that have not been able to be characterized so far.⁷ Crabtree was able to identify iridium dihydride complexes by ^1H and ^{31}P NMR spectroscopy, after treating $[(\text{PR}_3)(\text{pyridine})\text{-Ir}(\text{COD})]\text{PF}_6$ with H_2 .⁸ He also presented evidence that these dihydrides are intermediates in the catalytic hydrogenation of cyclooctadiene. However, no experimental information about the catalytic cycle and the intermediates involved in the hydrogenation of simple alkenes is available. Therefore, the mechanism of iridium-catalyzed asymmetric hydrogenation and the nature of the enantioselective step remain elusive.

Recently, Brandt et al. published a computational study in which they proposed a catalytic cycle via Ir(III) and Ir(V) intermediates generated by addition of two molecules of H_2 to the Ir(I) center. Their conclusion was based on density functional theory (DFT) calculations of various potential reaction pathways, using $\text{Me}_2\text{PCH}=\text{CHCH}=\text{NMe}$ as a truncated achiral model for the PHOX ligand and ethylene as substrate.⁹ This approach seems problematic because, in Ir(PHOX) complexes bearing a coordinated trisubstituted olefin, steric interactions must be very important and, therefore, the relative energies of the sterically much less demanding model complexes do not necessarily parallel those of the full structures.

Further experimental as well as computational work will be necessary to establish a credible mechanism that explains the observed enantioselectivities. As a first step in this direction we carried out a combined experimental and computational study of the reaction of the Ir(PHOX) complex **1a** with H_2 . Here we report the results, which show that the addition of H_2 is highly stereoselective as a result of steric and electronic effects exerted by the PHOX ligand. Quantum mechanical calculations

at the DFT level, which included the complete PHOX ligand structure, were consistent with experimental data, indicating that it should be possible to explore potential reaction sequences of the entire catalytic cycle by high-level calculations of the full catalyst and substrate structures.

Computational Methods

All ab initio calculations were carried out using the GAUSSIAN03 suite of programs at the DFT level with the LANL2DZ effective core potential for iridium, while all other atoms were treated with explicit basis sets of 6-31G(d,p) quality.¹⁰ Calculations started from a guess of the wave function at the Hartree–Fock level and improvement of the wave function until the level described was reached. To integrate the density functional, the grid = ultrafine option was used. This choice proved to be crucial to reproduce results from the literature.^{11,12} Then, structural optimizations followed that converged the total energy to better than $10^{-7}E_{\text{h}}$. Addition of further polarization functions to the Ir and P atoms did not appreciably change the results reported below. To limit the computational effort, they were not included in the final basis set.

To establish the validity of the approach chosen here, test calculations were carried out. The systems included $[\text{Ir}(\text{H})_2(\text{P}^i\text{Bu}_2\text{Ph})_2]^+$ and $[(\text{C}_5\text{H}_5)\text{-Ir}(\text{PH}_3)]$.^{11,12} For the first iridium complex results from previous ab initio calculations along with structural data were available, while for the second complex detailed information on the coordinates has been published. The basis set and methods used here show good agreement compared to the B3LYP/LANL2DZ(Ir,P)/valence double- ζ calculations on $[\text{Ir}(\text{H})_2(\text{P}^i\text{Bu}_2\text{Ph})_2]^+$, in particular for the Ir–P and Ir–H distances and the Ir–P–C angles. For $[(\text{C}_5\text{H}_5)\text{Ir}(\text{PH}_3)]$ the optimized structures are virtually identical to the published data for both the singlet and the triplet states. Furthermore, the energetics is described correctly since the calculated energy difference of 9.1 kcal/mol between the two electronic states compares favorably with 8.4 kcal/mol from the literature.

Results and Discussion

Hydrogenation Experiments. For our combined experimental and computational study we chose the structurally well characterized $[(\text{PHOX})\text{Ir}(\text{COD})]\text{BAR}_{\text{F}}$ complex **1a** we had previously used as a precatalyst in several synthetic and kinetic studies.^{1,2,13} Initial attempts to follow the reaction with H_2 under standard conditions by NMR spectroscopy failed. When H_2 was added to a CD_2Cl_2 solution of complex **1a** in an NMR tube, the spectrum showed a complex mixture of hydrido complexes which could not be analyzed. However, when a more strongly coordinating solvent such as $[\text{D}_8]\text{THF}$ was used, three dihydroiridium complexes could be identified and characterized by

- (5) For studies of hydrido(diphosphine)iridium complexes and their reactivity toward functionalized olefins, see: (a) Alcock, N. W.; Brown, J. M.; Derome, A. E.; Lucy, A. R. *J. Chem. Soc., Chem. Commun.* **1985**, 575–578. (b) Alcock, N. W.; Brown, J. M.; Maddox, P. J. *J. Chem. Soc., Chem. Commun.* **1986**, 1532–1534. (c) Brown, J. M.; Maddox, P. J. *J. Chem. Soc., Chem. Commun.* **1987**, 1276–1278. (d) Brown, J. M.; Maddox, P. J. *J. Chem. Soc., Chem. Commun.* **1987**, 1278–1280. For kinetic and thermodynamic studies of $[(\text{diphosphine})\text{Ir}(\text{COD})]\text{BF}_4$ complexes and their reactivity toward molecular hydrogen, see: (e) Kimmich, B. F. M.; Somsook, E.; Landis, C. R. *J. Am. Chem. Soc.* **1998**, *120*, 10115–10125. (f) Landis, C. R.; Brauch, T. W. *Inorg. Chim. Acta* **1998**, *270*, 285–297.
- (6) (a) Brown, J. M.; Chaloner, P. A. *Tetrahedron Lett.* **1978**, *21*, 1877–1880. (b) Brown, J. M.; Chaloner, P. A. *J. Chem. Soc., Chem. Commun.* **1980**, 344–346. (c) Brown, J. M.; Parker, D. *Organometallics* **1982**, *1*, 950–956. (d) Halpern, J. *Science* **1982**, *217*, 401–407. (e) Chan, A. S. C.; Pluth, J. J.; Halpern, J. *J. Am. Chem. Soc.* **1980**, *102*, 838–840. (f) Chan, A. S. C.; Pluth, J. J.; Halpern, J. *J. Am. Chem. Soc.* **1980**, *102*, 5952–5954. (g) Landis, C. R.; Halpern, J. *J. Am. Chem. Soc.* **1987**, *109*, 1746–1754. (h) Landis, C. R.; Feldgus, S. *Angew. Chem., Int. Ed.* **2000**, *39*, 2863–2866. (i) Feldgus, S.; Landis, C. R. *J. Am. Chem. Soc.* **2000**, *122*, 12714–12727.
- (7) More stable hydrido complexes with additional strong ligands such as $[(\text{PHOX})\text{Ir}(\text{H})_2(\text{PPh}_3)\text{Cl}]$ or $[(\text{PHOX})\text{Ir}(\text{H})_2(\text{TMEDA})]^+$ have recently been characterized: (a) Carmona, D.; Ferrer, J.; Lorenzo, M.; Santander, M.; Ponz, S.; Lahoz, F. J.; Lopez, J. A.; Oro, L. A. *Chem. Commun.* **2002**, 870–871. (b) Drago, D.; Pregosin, P. S.; Pfaltz, A. *Chem. Commun.* **2002**, 286–287.
- (8) (a) Crabtree, R. H.; Felkin, H.; Fillbeen-Kahn, T.; Morris, G. E. *J. Organomet. Chem.* **1979**, *168*, 183–195. (b) Crabtree, R. H.; Uriarte, R. J. *Inorg. Chem.* **1983**, *22*, 4152–4154. (c) Crabtree, R. H.; Demou, P. C.; Eden, D.; Mihelic, J. M.; Parnell, C. A.; Quirk, J. M.; Morris, G. E. *J. Am. Chem. Soc.* **1982**, *104*, 6994–7001.
- (9) Brandt, P.; Hedberg, C.; Andersson P. *Chem.–Eur. J.* **2003**, *9*, 339–347.

- (10) Frisch, M. J.; Trucks, G. W.; Schlegel, H. B.; Scuseria, G. E.; Robb, M. A.; Cheeseman, J. R.; Montgomery, J. A., Jr.; Vreven, T.; Kudin, K. N.; Burant, J. C.; Millam, J. M.; Iyengar, S. S.; Tomasi, J.; Barone, V.; Mennucci, B.; Cossi, M.; Scalmani, G.; Rega, N.; Petersson, G. A.; Nakatsuji, H.; Hada, M.; Ehara, M.; Toyota, K.; Fukuda, R.; Hasegawa, J.; Ishida, M.; Nakajima, T.; Honda, Y.; Kitao, O.; Nakai, H.; Klene, M.; Li, X.; Knox, J. E.; Hratchian, H. P.; Cross, J. B.; Adamo, C.; Jaramillo, J.; Gomperts, R.; Stratmann, R. E.; Yazyev, O.; Austin, A. J.; Cammi, R.; Pomelli, C.; Ochterski, J. W.; Ayala, P. Y.; Morokuma, K.; Voth, G. A.; Salvador, P.; Dannenberg, J. J.; Zakrzewski, V. G.; Dapprich, S.; Daniels, A. D.; Strain, M. C.; Farkas, O.; Malick, D. K.; Rabuck, A. D.; Raghavachari, K.; Foresman, J. B.; Ortiz, J. V.; Cui, Q.; Baboul, A. G.; Clifford, S.; Cioslowski, J.; Stefanov, B. B.; Liu, G.; Liashenko, A.; Piskorz, P.; Komaromi, I.; Martin, R. L.; Fox, D. J.; Morokuma, K.; Voth, G. A.; Peng, C. Y.; Nanayakkara, A.; Challacombe, M.; Gill, P. M. W.; Johnson, B.; Chen, W.; Wong, M. W.; Gonzalez, C.; Pople, J. A. *Gaussian 03*, revision B.01; Gaussian Inc.: Pittsburgh, PA, 2003.
- (11) Ujaje, G.; Cooper, A. C.; Maseras, F.; Eisenstein, O.; Caulton, K. G. *J. Am. Chem. Soc.* **1998**, *120*, 361–365.
- (12) Smith, K. M.; Poli, R.; Harvey, J. N. *Chem.–Eur. J.* **2001**, *7*, 1679–1690.
- (13) (a) Blackmond, D. G.; Lightfoot, A.; Pfaltz, A.; Rosner, T.; Schnider, P.; Zimmermann, N. *Chirality* **2000**, *12*, 442–449. (b) Smidt, S. P.; Zimmermann, N.; Studer, M.; Pfaltz, A. *Chem.–Eur. J.*, in press (review only).

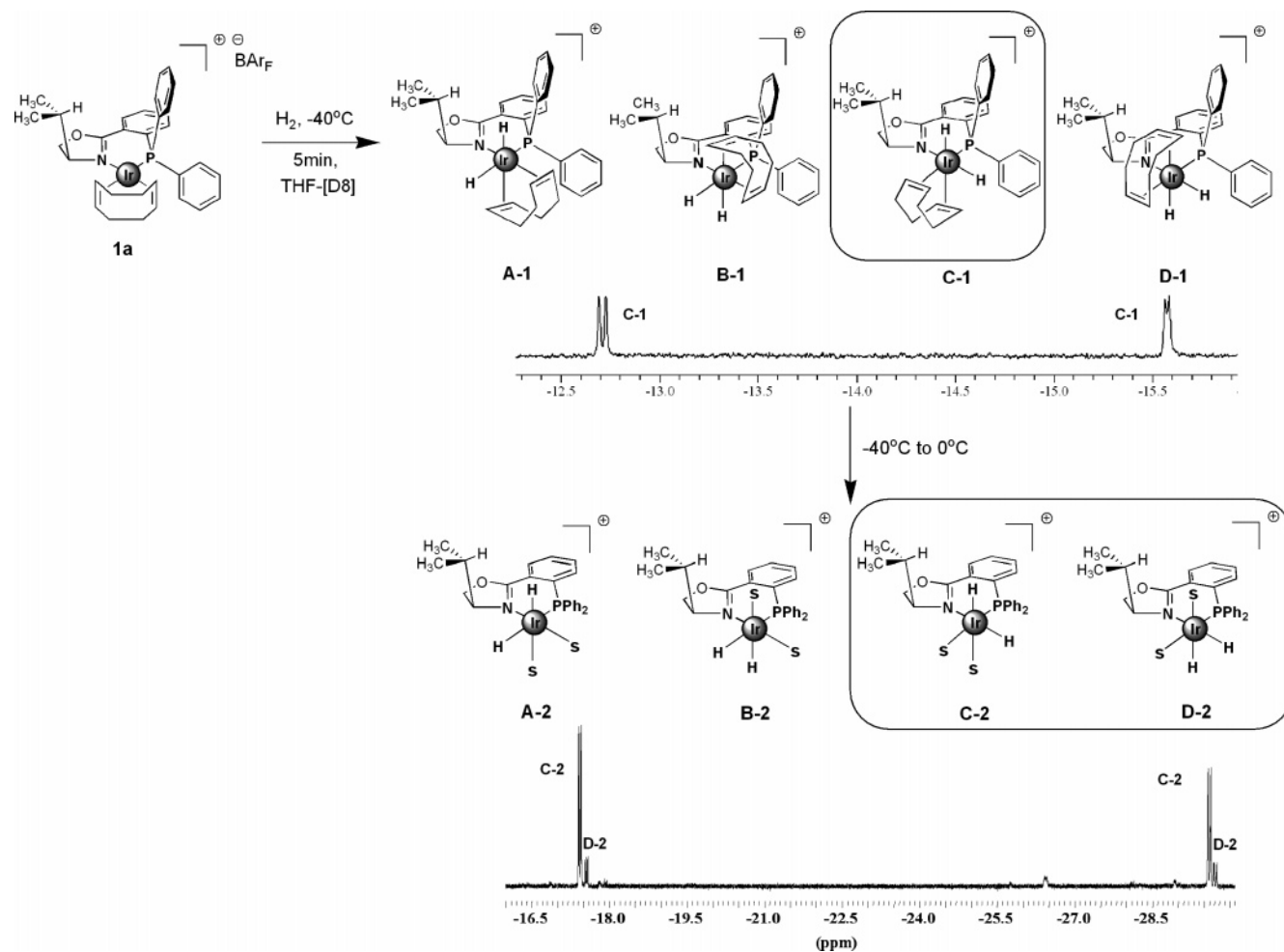


Figure 1. Reaction sequence of $[(PHOX)Ir(COD)]BARF$ with molecular hydrogen. In each step, the four possible isomers arising from *cis* addition of molecular hydrogen are depicted. The frames indicate the observed species, along with the corresponding 1H NMR signals in the hydride region. For clarity, the counterions are omitted for the dihydro intermediates ($BARF$ = tetrakis[3,5-bis(trifluoromethyl)phenyl]borate; s = THF).

one- and two-dimensional low-temperature NMR experiments (Figure 1). After hydrogen was bubbled through a solution of **1a** in the NMR tube at $-40^\circ C$ for 5 min, two new signals appeared in the hydride region that were assigned to a single dihydride complex formulated as $[(PHOX)Ir(H)_2(COD)]BARF$.

In principle, four diastereomeric *cis*-dihydride addition products can be formed (Figure 1, structures **A-1**, **B-1**, **C-1**, and **D-1**). Remarkably, only one of the four possible diastereomers was observed. No signals of other hydride complexes could be detected in the 1H NMR spectra above the noise level, indicating that the major isomer dominates over the others by a factor of >100 . Furthermore, no spectral changes were observed upon slowly warming the solution from -40 to $0^\circ C$ within 45 min, indicating that the kinetically preferred product of H_2 addition is also thermodynamically favored.^{5e,14,15}

The $^2J(H,P)$ values of 20 Hz clearly showed that both hydrides were disposed *cis* to the phosphorus atom. For a *trans* arrangement as in **A-1** and **B-1** larger coupling constants of 150–200 Hz would be expected.¹⁶ Discrimination between isomers **C-1** and **D-1** was possible by two-dimensional NMR experiments. Observation of NOE contacts between the hydride

in the apical position (H1) and the isopropyl substituent (H3), as well as the *ortho* proton of one of the *P*-phenyl rings (H5), are consistent with structure **C-1**, whereas in isomer **D-1** the two hydrides are clearly outside the NOE range of the isopropyl group. A three-dimensional model of isomer **C-1** based on the NMR data is depicted in Figure 2. The model is consistent with NOEs observed between protons H1 and H3, H1 and H4, H1 and H5, H1 and H8, H2 and H4, H2 and H6, and H2 and H7.

The observed, highly selective formation of isomer **C-1** results from H_2 addition to the more sterically encumbered face of the starting complex **1a**. The high preference for this pathway over the alternative pathway leading to complex **D-1** is likely due to steric factors. Dihydrogen addition to the sterically more accessible face, leading to isomer **D-1**, would build up steric strain between the chelating COD ligand and the isopropyl group in the oxazoline ring and the pseudoaxial *P*-phenyl group. The predominance of isomer **C-1** over isomer **A-1** or **B-1** is consistent with Crabtree's findings, who convincingly demonstrated that in the reaction of H_2 with $[(PR_3)(pyridine)Ir(COD)]PF_6$

(14) Bailar, J. C. J. *Inorg. Nucl. Chem.* **1958**, *8*, 165–175.

(15) For a related study of Ir complexes with *P,S*-ligands, see: Evans, D. A.; Michael, E. F.; Tedrow, J. S.; Campos, K. R. *J. Am. Chem. Soc.* **2003**, *125*, 3534–3543.

(16) (a) Parish, R. V. *NMR; NQR; EPR and Mössbauer Spectroscopy in Inorganic Chemistry*; Ellis Horwood Ltd.: New York, 1990. (b) Jesson, J. P. In *Transition Metal Hydrides*; Muetterties E. L., Ed.; Marcel Dekker: New York, 1971; pp 75–201. (c) Green, M. L. H.; Jones, D. J. In *Advances in Inorganic Chemistry and Radiochemistry*; Emeleus, H. J., Sharpe, A. G., Eds.; Academic Press: New York, 1965; Vol. 7, p 286.

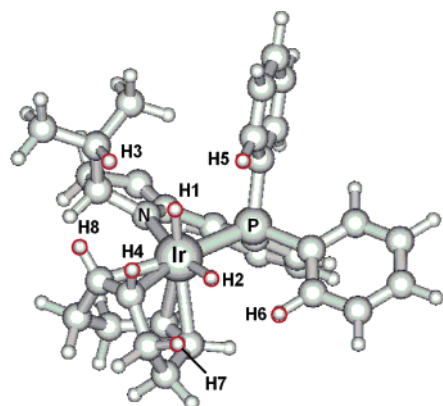


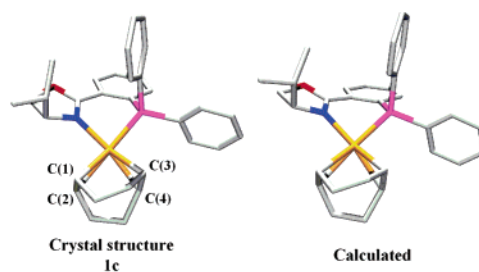
Figure 2. Three-dimensional model of isomer **C-1** based on NMR analysis. Protons identified by NOEs are labeled in red.

the formation of an Ir–H bond *trans* to the N ligand is electronically favored.⁸ In summary, our findings demonstrate that the remarkable stereoselectivity of H₂ addition is the result of both steric and electronic factors.

When the solution containing complex **C-1** was warmed to 0 °C under hydrogen, and kept at that temperature for 30 min, gradual consumption of isomer **C-1** was observed, accompanied by the appearance of two new hydride complexes, **C-2** and **D-2**, with concomitant formation of free cyclooctane. The structures of these complexes were established by two-dimensional NMR spectroscopy (Figure 1, bottom). The same products were also obtained directly from complex **1a** by bubbling hydrogen gas through a THF solution at 0 °C for 1–2 h. However, even when the experimental conditions were reproduced scrupulously, a different product ratio was observed each time. This observation indicates that the reaction is not under thermodynamic control.

The low chemical shifts as well as the ²J(H,P) values (20 Hz) indicate that both hydrides in the two isomers **C-2** and **D-2** are coordinated *cis* to the P atom. As in complex **C-1** a *trans*-(N–Ir–H) arrangement is favored over the *cis* arrangement. The highly negative chemical shift of one signal of each isomer (approximately –29 ppm) is consistent with one hydride coordinated *trans* to a weak ligand (i.e., a solvent molecule).^{8c} Furthermore, the formation of complex **D-2** indicates that H₂ addition to the sterically less encumbered face is possible in the absence of additional sterically demanding ligands such as COD. Prolonged reaction at room temperature leads to the formation of trimeric hydride complexes, as observed in earlier work.¹⁷ It is known that in the absence of coordinating olefins (hydrido)Ir(PHOX) complexes irreversibly form stable, catalytically inactive trimers, rendering structural studies of these species very difficult. In contrast, analogous hydrido(diphosphine) complexes such as [Ir(H)₂(solvent)₂(PR₃)₂]⁺ are more stable and could be isolated under a hydrogen atmosphere.¹⁸

Computational Studies. The NMR experiments summarized in Figure 1 show how the precatalyst **1a** is activated by oxidative addition of H₂ and how the stereochemistry of this process is controlled by the chiral ligand. Complexes **C-2** and **D-2** are potential intermediates in the catalytic cycle, if the reaction follows the so-called “hydride route” that proceeds through



	1a	1c	B3LYP
Ir–P	2.27(4)	2.26(4)	2.34
Ir–N	2.12(1)	2.09(7)	2.13
Ir–C(1)	2.20(6)	2.24(6)	2.27
Ir–C(2)	2.21(2)	2.22(5)	2.24
Ir–C(3)	2.13(7)	2.14(2)	2.17
Ir–C(4)	2.12(8)	2.13(1)	2.18
P–Ir–N	84.96	85.90	85.8

Figure 3. Comparison of selected experimental structural parameters of complexes **1a**^{21b} and **1c**^{21a} with the corresponding calculated values (distances between Ir and the coordinating atoms (Å), angle (deg) between the P–Ir and Ir–N bonds). H atoms are omitted for clarity.

dihydrido solvent complexes, which in a subsequent step react with the olefin.¹⁹ However, attempts to gain information about other possible intermediates involved in the catalytic cycle by NMR spectroscopy have failed so far. Therefore, we decided to carry out computational studies of Ir(PHOX) catalysts using ab initio quantum mechanical calculations to gain mechanistic insight complementary to the experimental results. Because steric effects obviously play a major role in these systems, we decided to retain the full complexity of the molecules rather than to resort to simpler model compounds, despite the substantially longer computing time required for such relatively complex structures. As mentioned in the Computational Methods, the reliability of B3LYP/LANL2DZ was established by comparison with previously reported calculations.^{11,12} To further test the reliability of the chosen method, the structure of complex **1c** was calculated and compared with experimental data from two crystal structure analyses. Calculations were carried out with the B3LYP parametrization of the exchange–correlation functional since this has proven to give reliable results for structures and energies^{11,12,20} of iridium-containing systems. As shown in Figure 3, the calculated structure agrees well with two crystal structures of the PF₆[–] (**1c**) and BARF[–] (**1a**) salts determined by X-ray analysis.²¹

The largest deviations from experimental data (0.07 and 0.08 Å) are found for the Ir–P bonds. The *trans* influence, resulting in longer Ir–C distances for the C=C bond coordinated *trans* to the P atom compared to the C=C bond *trans* to the N atom, is well reproduced, as seen from the Ir–C(1) and Ir–C(2) distances, which are longer than the Ir–C(3) and Ir–C(4)

(17) Smidt, S. P.; Pfaltz, A.; Martínez-Viviente, E.; Pregosin, P. S.; Albinati, A. *Organometallics* **2003**, *22*, 1000–1009.

(18) (a) Crabtree, R. H.; Hlatky, G. G.; Parnell, C. A.; Segmueller, B. E.; Uriarte, R. J. *Inorg. Chem.* **1984**, *23*, 354–358. (b) Crabtree, R. H.; Mellea, M. F.; Mihelcic, J. M. *Inorg. Synth.* **1990**, *28*, 56–60.

(19) (a) Halpern, J.; Riley, D. P.; Chan, A. S. C.; Pluth, J. J. *J. Am. Chem. Soc.* **1977**, *99*, 8055–8057. (b) Brown, J. M. In *Comprehensive Asymmetric Catalysis*; Jacobsen, E. N., Pfaltz, A., Yamamoto, H., Eds.; Springer-Verlag: Berlin, 1999; Vol. 1, pp 122–182. (c) Heinrich, H.; Giernoth, R.; Bargon, J.; Brown, J. M. *Chem. Commun.* **2001**, 1296–1297.

(20) Blum, O.; Carmielli, R.; Martin, J. M. L.; Milstein, D. *Organometallics* **2000**, *19*, 4608–4612.

(21) (a) Schneider, P.; Koch, G.; Prétôt, R.; Wang, G.; Bohnen, F. M.; Krüger, C.; Pfaltz, A. *Chem.–Eur. J.* **1997**, *3*, 887–892. (b) Smidt, S. P. Dissertation, University of Basel, Basel, Switzerland, 2003. (The crystal structure of compound **1a** was submitted to the CCDB with number 201702.)

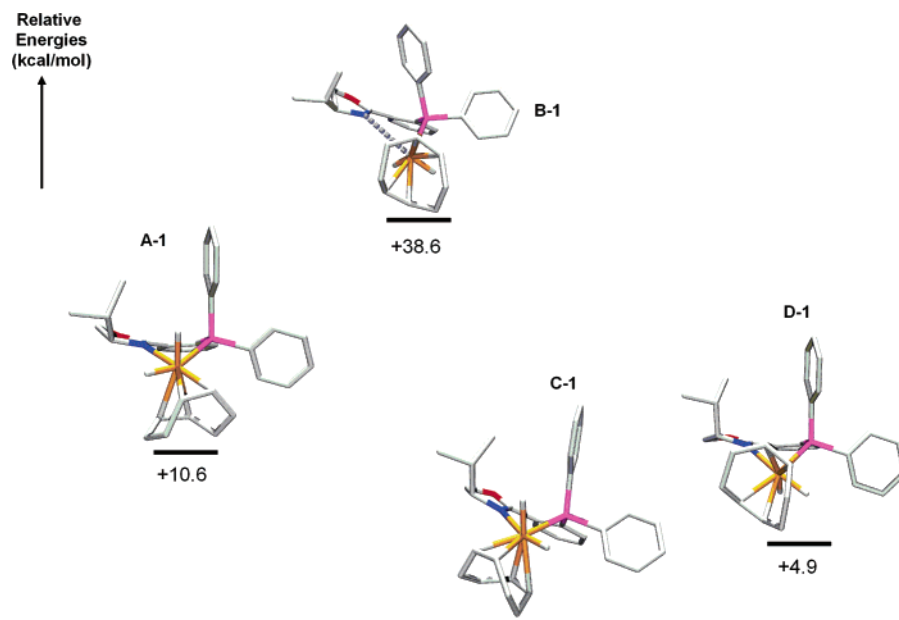


Figure 4. Calculated structures and relative energies of $[(\text{PHOX})\text{Ir}(\text{H})_2(\text{COD})]^+$ complexes. For reasons of clarity, the protons of the ligand and of the cyclooctadiene moiety are not shown.

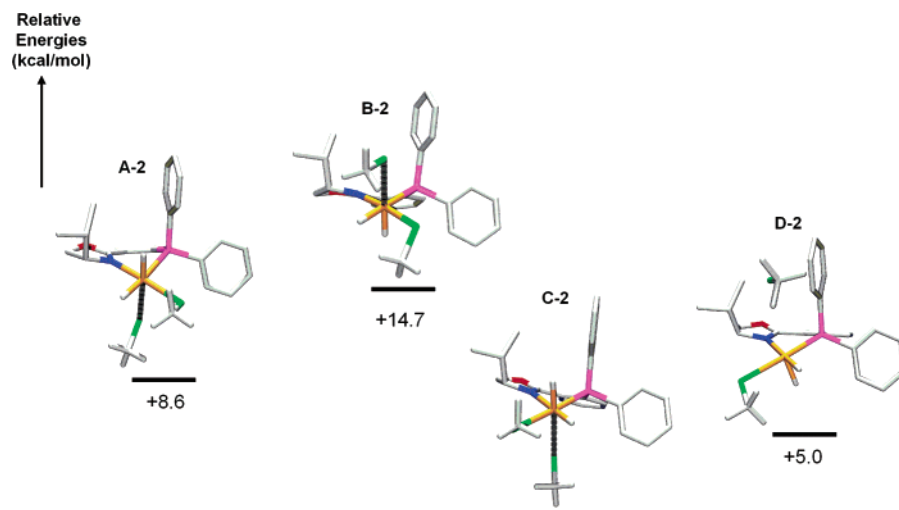


Figure 5. Calculated structures and relative energies of $[\text{Ir}(\text{PHOX})(\text{H})_2(\text{solvent})_2]^+$ complexes. H atoms of the ligand backbone are omitted for clarity.

distances by approximately 0.1 Å. The calculated N–Ir–P angle closely matches the experimentally determined values. Furthermore, the overall geometry of the complex, including the orientation of the isopropyl substituent and the *P*-phenyl rings, is well reproduced by the DFT approach.

After having established that our computational approach provided realistic structural data for complex **1a**, we calculated the fully minimized structures of the four possible *cis*-dihydride complexes, which can be formed by H₂ addition to the $[(\text{PHOX})\text{Ir}(\text{COD})]^+$ complex. As shown in Figure 4, the computed relative energies of the four isomers differ substantially. The most stable calculated structure **C-1** corresponds to the reaction product that was shown to be formed exclusively in the NMR experiment (Figure 1). The significant energy difference between **C-1** and **D-1** can be explained by unfavorable steric interactions of the COD ligand with the oxazoline moiety. In contrast, the higher stability of isomer **C-1** compared to **A-1** is likely due to the electronically favored coordination of a hydride *trans* to the N atom.⁸ Isomer **B-1** was not found. The geometry search

of the potential energy surface led to a chemically irrelevant minimum depicted in Figure 1. The unusually long Ir–N distance (3.51 Å) reflects the strong steric repulsion between the oxazoline moiety and the COD ligand. Electronic effects as well (H *trans* to P) probably destabilize the hypothetical structure **B-1**. The computed energies indicate that the experimentally observed product of H₂ addition is the thermodynamically most stable isomer. The results also show that the PHOX ligand can efficiently control the geometry of Ir–hydride complexes.

Next, the four possible $[(\text{PHOX})\text{Ir}(\text{H})_2(\text{solvent})_2]^+$ complexes, resulting from hydrogenation and subsequent dissociation of the COD ligand, were studied. To simulate the presence of dichloromethane, which is used as a solvent in the asymmetric hydrogenation, two coordinating molecules of methyl chloride were included in the calculations. The relative energies of the four isomers follow the same order as those of the analogous dihydrido(COD) complexes (Figure 5). The most notable difference is the much lower energy gap between the least stable

isomer **B-2** and the other isomers, compared to the COD complex **B-1** that is strongly destabilized by steric interactions of the COD with the PHOX ligand. The solvent molecule in a pseudoapical position in **D-2** only interacts very weakly with the iridium atom (Ir–Cl distance of 5.95 Å), probably as a result of steric interferences with the bulky groups of the PHOX ligand. The lowest energy structure **C-2** corresponds to the major isomer formed in the NMR experiment.

Complex **D-2**, which corresponds to the minor isomer observed experimentally, is 5.0 kcal/mol less stable than **C-2**, while the other two structures, **A-2** and **B-2**, are 8.6 and 14.7 kcal/mol higher in energy. When comparing the experimental with the computational results, one should keep in mind that the NMR experiment was carried out in THF, which is a strongly coordinating solvent, whereas in the calculations methyl chloride was used as a coordinating solvent. Therefore, the relative energies of the complexes observed in THF and the computed values may differ substantially. Nevertheless, the results demonstrate that the computational approach used leads to experimentally meaningful structures.

Experimental Section

In a glovebox, the iridium complex was weighed into an NMR tube, which was then filled with deuterated solvent under an argon atmosphere and put in a long narrow Schlenk tube sealed with a rubber septum. The sample was then thermostated at the desired temperature. A cooling mantle filled with dry ice was placed around the upper part of the Schlenk to avoid evaporation of the deuterated solvent. Hydrogen gas (quality >99.99%) was introduced through a long stainless steel needle. The needle was attached to a three-way stopcock, allowing the whole apparatus to be purged by three argon-vacuum cycles before switching to hydrogen. The gas was bubbled through the solution at flow rates between 2 and 5 mL/min. The NMR tube was finally sealed with a rubber septum and introduced into the NMR spectrometer (Bruker Avance 500) precooled to the desired temperature.

Conclusion

The experimental observation of a single [(PHOX)Ir(H)₂(COD)]⁺ isomer, **C-1**, as the primary product in the hydrogenation of the [(PHOX)Ir(COD)]⁺ precursor **1a** clearly shows that

the chiral phosphinooxazoline ligand effectively controls the stereochemistry of H₂ addition. The next steps as well, which lead to [(PHOX)Ir(H)₂(solvent)₂]⁺ complexes **C-2** and **D-2** with concomitant loss of COD, are controlled by the chiral ligand. The stereoselectivity in these reactions can be explained by steric effects of the PHOX ligand combined with a strong electronic influence of the coordinating N and P atoms, favoring addition of a hydride *trans* to the oxazoline ring. DFT calculations of the structures and energies of the possible stereoisomers of [(PHOX)Ir(H)₂(COD)]⁺ and [(PHOX)Ir(H)₂(solvent)₂]⁺ complexes showed that the computational methods chosen lead to experimentally meaningful results. The substantial energy differences between the different isomers clearly demonstrate that steric interactions are very important in these complexes. Thus, any computational evaluation of potential catalytic intermediates and reaction pathways should include full structures of the chiral ligand and the substrate. Our results show that this is in principle possible, although the relatively complex structures of Ir(PHOX) complexes require substantial computational efforts. As a next step in this direction, we are currently extending our calculations to other (hydrido)Ir(PHOX) complexes that could play a role as potential intermediates in the Ir-catalyzed asymmetric hydrogenation.

Acknowledgment. The ab initio calculations were carried out with generous allocation of computing time on machines of the Swiss Center for Scientific Computing (SCSC), Manno, Switzerland. Financial support from the Swiss National Science Foundation (SNSF) is gratefully acknowledged. S.P.S. thanks the Gottlieb Daimler- and Carl Benz-Foundation and the German Academic Exchange Service (DAAD). M.M. acknowledges support from the SNSF through a Förderungsprofessur. We thank one of the reviewers for helpful suggestions and comments.

Supporting Information Available: Experimental procedure and NMR characterization (PDF). This material is available free of charge via the Internet at <http://pubs.acs.org>.

JA046318Z